Control of Steering and Brake Actuator Dynamics in Driverless Vehicles: A Real-World Formula SAE Skid-Test Scenario

Danilo MENEGATTI*, Francesco PAPPALARDO, Francesco LUZI, and Alessandro GIUSEPPI

***Abstract*— Autonomous driving has emerged as a technology to revolutionize the future of transportation and completely re-define the landscape of road systems. Accurate control algorithms are crucial to ensure the safety and efficiency of autonomous vehicles; in particular, incorporating actuator dynamics into the vehicle dynamics model can improve the response of the system to control commands, with clear safety implications. This work proposes pulse width modulation-based control strategies for the steering and brake actuators of a Formula SAE driverless vehicle. Extensive simulation tests and real-world experiments on a Formula SAE skid-test scenario validate the proposed approach.**

***Index Terms*— Autonomous Driving, Actuator Dynamics, Intelligent Control**

I. INTRODUCTION

Autonomous driving represents one of the most promising advancements in modern technology, with the potential to significantly enhance transportation efficiency, safety, and accessibility. Self-driving vehicles leverage real-time data processing algorithms together with advanced control techniques to navigate complex environment with little to no human interaction. From a functional point of view, autonomous vehicles consist of two main components, one of environmental awareness, and the other of control algorithms designed to solve path planning and path tracking problems, which involve determining the optimal route to reach a destination and following it while ensuring road safety. The removal of the human element in the driving process, is an innovation that promises to enhance road safety, reduce traffic congestion, and lead towards sustainable transportation systems and any development and enabling technology that closes the gap towards fully autonomous driving is hence of the utmost importance for the development of society as a whole.

To achieve precise and accurate control, control algorithms require detailed information about the dynamic behaviour of autonomous vehicles, mathematically described through a dynamical model. In this context, it is essential to explicitly consider the dynamics of actuators, as they are components that directly influence the vehicle's response to control inputs. By leveraging on their modelled dynamics, control algorithms can be more accurate in prediction and in the steering the vehicle dynamics towards an optimal behaviour. This approach enhances the vehicle's ability to handle real-world driving scenarios, leading to smoother and safer maneuvers.

The authors are with the Department of Computer, Control and Management Engineering "Antonio Ruberti" – Sapienza University of Rome.

*Corresponding author. Email: menegatti@diag.uniroma1.it

This work focuses on a hierarchical control scenario of an autonomous vehicle, explicitly referring to the control of steering and brake actuators, respectively. Extensive validation is performed over simulation tests and a real-world Formula SAE skid-test scenario, leveraging the Sapienza Fast Charge Formula SAE Electric Racing Team models.

The main contributions of this work are:

- Formulation of a control strategy to explicitly deal with actuators dynamics
- Implementation of a hierarchical control scheme employing PWM signals
- Building of a real-world control platform based on a ESP32 microcontroller and CAN bus module
- Evaluation of the proposed approach over a real-world Formula SAE skid-test scenario

The remainder of the manuscript is organized as follows: Section II discusses some related works; Section III illustrates the overall system architecture; Section IV provides a detailed description of the proposed control paradigm; Section V presents the simulation results, highlighting the high its effectiveness in real-world scenarios; Section VI draws the conclusions and outlines future research work.

II. RELATED WORKS

In the context of autonomous vehicles, actuator include components such as motors, brakes, and steering mechanisms, whose dynamic behaviour directly affects that of the vehicle, namely how it reacts to control input. Therefore, they play an important role within the path tracking problem, that is to ensure the vehicle to follow a predefined trajectory by continuously adjusting its steering, acceleration and braking.

Geometric-based methods have been introduced for active front-wheel steering vehicles [1], [2] to solve the path tracking problem leveraging the geometry of the vehicle kinematics and the reference path by computing a set of look-ahead waypoints. Although their implementation is quite straightforward, they completely lack any information about the vehicle dynamics. To account for this issue, model-based approaches have been preferred by the scientific community over time.

A valid alternative to geometric approaches is represented by Proportional Integral Derivative Controllers (PIDs) which rely on a model describing the system dynamics and require tuning of only three parameters, thereby avoiding excessive complexity; [3] represents one of the first works to employ a PID controller within the scope of a path tracking problem. In particular, the authors of [4] developed a nested control scheme, with the inner control loop based on a PI controller,

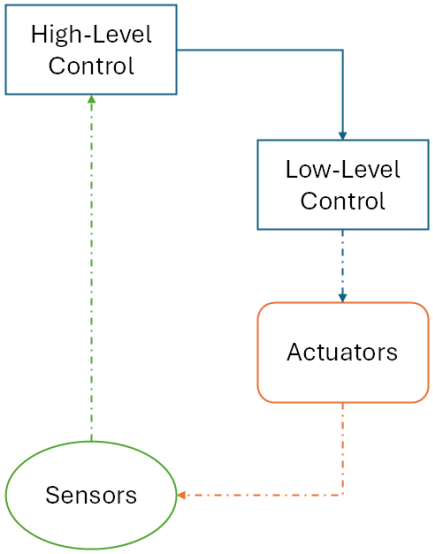

Fig. 1. Proposed hierarchical control scheme; the high-level controller interacts with sensors and outputs reference signals for the low-level control, which interacts with the actuators.

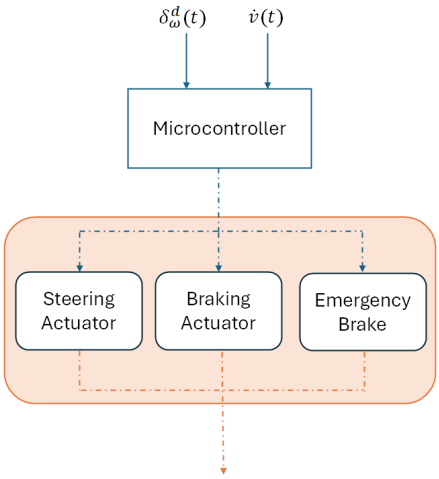

Fig. 2. Detailed diagram of the interaction between the low-level controller, referred to as "Microcontroller", and the three actuators considered, namely "Steering Actuator", "Braking Actuator", and "Emergency Brake".

while the outer one on a PID controller, with the aim to reduce the steering angle error and the lateral deviation from a predefined trajectory, respectively, while in [5] an adaptive PID controller was developed, showing superior performance in S-shaped trajectories. Along with lateral dynamics, PIDs were also employed to control the longitudinal dynamics, as in [6] where an adaptive controller is derived.

In addition to PIDs, fuzzy logic controllers have been utilized to manage the complexities and uncertainties in vehicle dynamics, offering a more flexible and adaptive approach to control. Leveraging a set of rules on the basis of which decisions are made, they have been employed in path tracking control by the authors of [7] and [8].

Sliding mode controllers represent another paradigm to tackle path tracking by steering and keeping the state of the autonomous vehicle to a predefined sliding surface, thus ensuring predefined performance. Such an approach is carried out by the authors of [9]–[11].

Although the above mentioned approaches proved to be very effective, they all lack the explicit inclusion of constraints in the problem formulation. This issue has been tackled via linear quadratic regulators, which aim to regulate the behaviour of the autonomous system by solving a constrained optimization problem; in [12] an iterative algorithm to tackle non-convex constraints is proposed, while the authors of [13] develop an approach which proves to be robust against noise and measurement errors.

Another approach which is suitable to deal with constraints explicitly is model predictive control which, leveraging a receding horizon strategy, is inherently robust to disturbances and uncertainties. It has been widely utilized to achieve both lateral and longitudinal control of the vehicle in [14] and [15], with the authors of [16] including a Kalman filter in the control loop to tackle the presence of obstacles.

Taking inspiration from model-based approaches that explicitly handle actuator constraints, this work aims to propose a hierarchical control paradigm for path tracking, which is based on the control of the dynamics of the steering and brake actuators, ensuring that the vehicle can accurately follow the desired trajectory.

III. System Architecture

The dynamical system to be controller is an autonomous four-wheel-drive vehicle with steering on the front wheels only. Autonomous driving is realised through a hierarchical control approach, with a high-level controller and a low-level controller responsible for two critical aspects of the overall process.

Figure 1 shows a high-level description of the proposed control paradigm. The high-level controller interfaces with the sensing level, receiving data from all sensors installed in the vehicle, such as cameras, LiDAR (Light Detection and Ranging) and GPS. This data is processed to determine the control actions required to navigate the vehicle. The control actions are then transmitted to the low-level controller, which converts them into appropriate signals to steer the actuators.

Assuming that the focus is on horizontal dynamics, thus neglecting roll, pitch and yaw, the vehicle can be described using the dual-track model [17]. Therefore, the high-level controller aims to handle later and longitudinal dynamics only. To this end, it is assumed to output signals such as steering angle and longitudinal acceleration. The low-level controller manipulates these signals to control the steering, brake and emergency brake actuators.

While the latter is a purely mechanical device that can be remotely actuated in the event of malfunctions or abnormal behaviour, the steering actuator consists of a stepper motor with a dedicated encoder flanked by a dedicated driver, while the brake actuator consists of a dedicated servomotor. At the hardware level, these actuators are managed by a microcontroller, as shown in Figure 2.

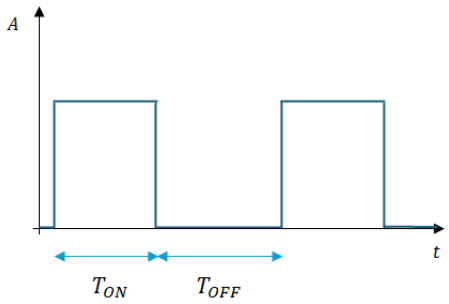

Fig. 3. Example of PWM signal; amplitude over time.

The stepper motor chosen for the steering actuator is a Nema 34E1K-45 Series P Closed Loop, a hybrid type motor having a mounting face of $3.4" \times 3.4"$, a step angle of 1.8, and a 1000 PPR position encoder included; it is governed by a Stepper Driver CL86T-V41, responsible for generating discrete electrical pulses that determine the rotor's movements. The choice of a hybrid stepper motor, with a rotor consisting of two polarized toothed wheels and the teeth offset by half a step between the two wheels, related to the division of the rotation into very small pitch angles, and a holding torque such that the rotor remains in a given position even in absence of current in the windings.

The brake actuator uses a DS51150 servomotor, capable of providing maximum torque of 173 Nm. The choice of this actuator, which includes a 12 V AC-powered motor, a reduction system with a series of gears to mechanically increase the torque of the motor output shaft, together with an encoder, is motivated by its small size and high torque.

Finally, the microcontroller responsible for receiving and manipulating the steering and acceleration signals from the high-level controller, in order to process a low-level control strategy, is an ESP32 WROOM 32. This microcontroller communicates with the other modules via CAN bus using a MCP2515 bus module.

IV. Pulse Width Modulation-based Actuator Control

Pulse Width Modulation is a digital control technique which allows to control electrical devices by means of a digital signal whose frequency and duty cycle can adjust at convenience. An example of a PWM signal is shown in Figure 3.

The frequency f is the inverse of the period T of the signal, which corresponds to the time between the start of one pulse and the start of the next one. This period includes two phases: the ON phase, during which the signal is active and assumes its minimum value. The duty cycle DC represents the percentage of time the signal is active relative to the total period.

Let T_{ON} and T_{OFF} represent the duration of the ON and OFF phases respectively, then $T = T_{ON} + T_{OFF}$, and frequency and duty cycle are defined as follows:

$$f = \frac{1}{T}, \qquad DC = \frac{T_{ON}}{T_{ON} + T_{OF}} \times 100. \qquad (1)$$

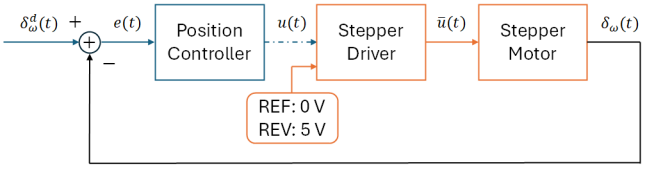

Fig. 4. Steering actuator's closed-loop control scheme.

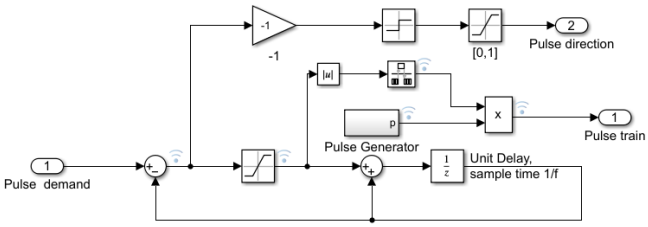

Fig. 5. Pulse Generator control scheme.

In the context of actuator control, frequency determines the speed of actuation, while the duty cycle influences the power or torque.

The steering actuator control scheme involves the microcontroller, the stepper driver, and the stepper motor, with the objective of adjusting the position of the motor shaft. This is achieved in a feedback fashion, as shown in Figure 4; the microcontroller (Position Controller), taking into account the error $e(t)$ between the steering angle $\delta^d_\omega(t)$ provided by the high-level controller and the actual steering angle $\delta_\omega(t)$, corresponding to the position of the motor shaft, generates a PWM signal $u(t)$ which the stepper driver translates into a voltage signal $\bar{u}(t)$ to steer the stepper motor.

At the core of the Position Controller there is a Pulse Generator, which takes as input the mismatch between the desired and actual steer angle, $e(t) = \delta^d_\omega(t) - \delta_\omega(t)$, to output the PWM signal and its corresponding direction via a bespoke control scheme, shown in Figure 5.

The error $e(t)$ is manipulated in parallel on two levels, one of which calculates the direction of the PWM signal by evaluating the sign of $e(t)$, while the other first calculates the absolute value of $e(t)$ so that frequency and duty cycle of the PWM signal are proportional to this value. Finally, additional manipulation is needed to make $u(t)$ coherent with the stepper driver module.

Upon receiving the PWM signal, the stepper driver generates two timing sequences, A and B, corresponding to voltage signals used to control the motor. With 0 V as the reference and 0.5 V as the threshold, the driver generates a step whenever the PWM signal exceeds the threshold. The reference signal is used to establish the quadrature between A and B; if the PWM signal is below the reference, A leads B, otherwise, B leads A.

Finally, on the basis of the signals received by the stepper driver, the stepper motor changes the position of its shaft, which correspond to a precise steer angle $\delta_\omega(t)$.

The brake actuator control involves the microcontroller

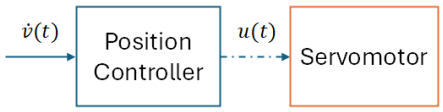

Fig. 6. Braking actuator's open-loop control scheme.

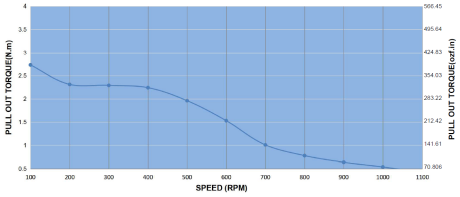

Fig. 7. Torque curve of the stepper motor in the optimal configuration.

and the servomotor, aiming to regulate the position of the latter' shaft, which corresponds to a given braking force, in an open-loop fashion, as shown in Figure 6; the microcontroller (Position Control) leverages the longitudinal acceleration signal $\dot{v}(t)$ coming from the high-level controller to derive a PWM signal on the basis of the same control paradigm as before, and the servomotor changes the position of its shaft accordingly.

V. Simulations

In order to validate the effectiveness of the proposed control approach, first simulation tests were conducted, followed by real-world experiments over the typical 8-shaped trajectory of Formula SAE' skid-pad tests, which aims to test the vehicle's performance in turns.

The simulation concerned the steering actuator and were aimed at finding the best stepper driver configuration, in terms of stepper motor supply voltage and PWM signal generation frequency, so as to make the transient behaviour of the stepper motor sufficiently short, as to make it suitable for the high-level controller's working frequency, set at 25 Hz.

For simulations purposes, the error $e(t)$, defined in terms of the steering angle, was considered directly in terms of steps according to the following conversion formula.

$$N = \mu \,\text{round}\left(\frac{\delta_\omega^d(t)\,\Gamma}{1.8}\right), \tag{2}$$

where $\mu = 1600$ represents the micro-stepping configuration, and Γ is a constant related to the gear ratio, as the steering angle $\delta_\omega(t)$ is related to that of the wheels $\theta_\omega(t)$ via the steering ratio Γ as follows:

$$\delta_\omega(t) = \frac{\theta_\omega(t)}{\Gamma}. \tag{3}$$

Simulations were carried out using Simulink [18] on an Intel Core i7 platform with 8 GB of RAM and Nvidia GeForce RTX 3060.

Extensive simulations were carried out, linearly varying the supply voltage of the stepper motor from 24 V up to 48 V, corresponding to the limit allowed by the Formula

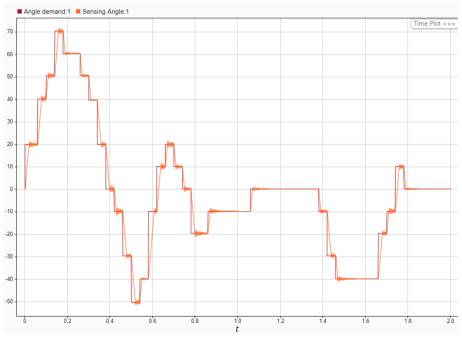

Fig. 8. Evolution of the stepper motor response (orange line) against changes in the steering angle (red line) over a simulated trajectory.

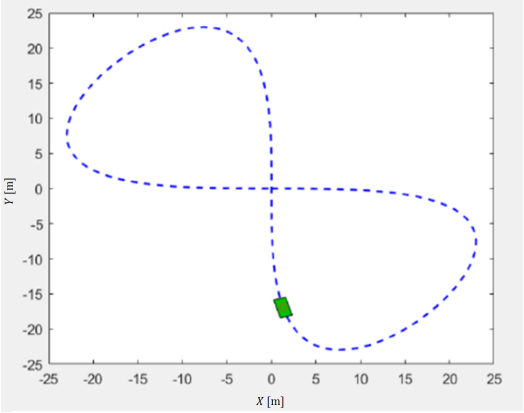

Fig. 9. Formula SAE 8-shaped skid test trajectory.

SAE regulation, as well as the frequency f of the PWM signal. As a result, the best configuration in terms of transient corresponds to a 48 V motor supply and a pulse rate of 2000, with a transmission ratio of 1:10 - the motor torque curve is shown in Figure 7. These simulations also made it possible to identify the gear ratio that would guarantee the best performance, from the original 1:7.5 to 1:10.

Once the best configuration was identified, the response of the steering actuator was simulated for time-varying values of the steering angle $\delta_\omega^d(t)$, replicating the inputs required for a certain trajectory. Figure 8 illustrates the stepper motor's response to changes in the steering angle, simulating the steering actuator's performance over a given trajectory; it is worth mentioning that the stepper motor successfully delivers a maximum torque of approximately 2.25 Nm.

Real-world experiments are conducted on the 8-shaped trajectory shown in Figure 9, where the vehicle starts from the (0,0) position and moves clockwise. The behaviour of the steering actuator is illustrated in Figure 10, where the blue line represents the desired steering angle $\delta_\omega^d(t)$ over time, and the yellow line represents the actual steering angle $\delta_\omega(t)$. In general, the actuator successfully replicates the desired behaviour, with a maximum error of $e_{MAX} = 2$.

Additional experiments have been performed with $\mu \in [1600; 6400]$. Even if the steering actuator speed increased from the 93.75 rpm for $\mu = 1600$, no practical advantages were observed.

With respect to the brake actuator, a potentiometer was

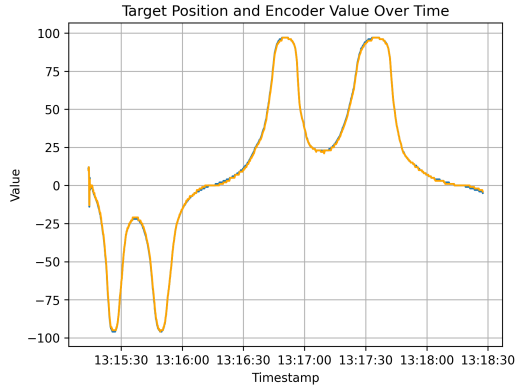

Fig. 10. Evolution of $\delta_\omega(t)$ (yellow line) against $\delta_\omega^d(t)$ (blue line) over the considered 8-shaped trajectory.

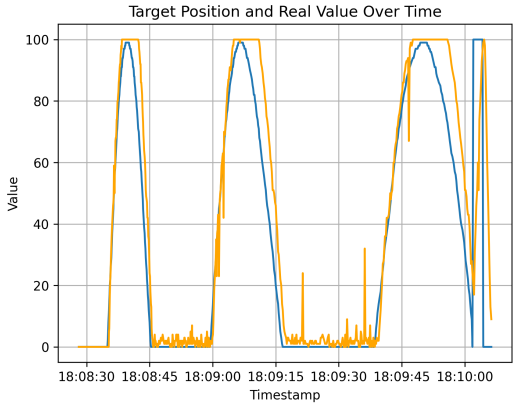

Fig. 11. Evolution of the actual braking force (yellow line) against desired one (blue line) over the considered 8-shaped trajectory.

used to map the servomotor's rotation angle in such a way an angle of 0° corresponds to a potentiometer value of 0, while an angle of -100° corresponds to a value of 100, representing the maximum braking force. The actuator's behaviour is shown in Figure 11, where the yellow line represents the actual braking force provided. Generally, high sensitivity to disturbances and noise was observed due to the use of the open-loop control; however, on average, the actuator is able to replicate the desired signal.

VI. Conclusions

This paper has presented a hierarchical PWM control approach for a real-life Formula SAE driverless vehicle, detailing a closed-loop approach for its steering, and an open-loop one for its braking actuators.

The former is based on the mismatch between the desired and actual steering angles, from which the frequency and direction of the PWM signal are derived using a bespoke proportional control scheme, while the latter directly utilizes the desired braking signal to generate a PWM signal. Extensive simulations tests and real-world experiments validate the proposed approach.

Future research work is aimed at improving the performance of both control schemes by introducing data-driven compensators, with the aim to handle nonlinearities and uncertainties.

Acknowledgment

The authors would like to thank Sapienza Fast Charge Formula SAE Electric Racing Team for the fruitful discussions which provided significant inputs for this work.

References

[1] C. Coulter, "Implementation of the pure pursuit path tracking algorithm," 1992.

[2] G. M. Hoffmann, C. J. Tomlin, M. Montemerlo, and S. Thrun, "Autonomous automobile trajectory tracking for off-road driving: Controller design, experimental validation and racing," in *2007 American Control Conference*, p. 2296–2301, IEEE, July 2007.

[3] F. A. A. Cheein, C. De La Cruz, T. F. Bastos, and R. Carelli, "Slam-based cross-a-door solution approach for a robotic wheelchair," *International Journal of Advanced Robotic Systems*, vol. 6, Jan. 2009.

[4] R. Marino, S. Scalzi, and M. Netto, "Nested pid steering control for lane keeping in autonomous vehicles," *Control Engineering Practice*, vol. 19, p. 1459–1467, Dec. 2011.

[5] P. Zhao, J. Chen, Y. Song, X. Tao, T. Xu, and T. Mei, "Design of a control system for an autonomous vehicle based on adaptive-pid," *International Journal of Advanced Robotic Systems*, vol. 9, Jan. 2012.

[6] A. Simorgh, A. Marashian, and A. Razminia, "Adaptive pid control design for longitudinal velocity control of autonomous vehicles," in *2019 6th International Conference on Control, Instrumentation and Automation (ICCIA)*, p. 1–6, IEEE, Oct. 2019.

[7] C. Hu, Y. Chen, and J. Wang, "Fuzzy observer-based transitional path-tracking control for autonomous vehicles," *IEEE Transactions on Intelligent Transportation Systems*, vol. 22, p. 3078–3088, May 2021.

[8] J. Zhang, L. Zhang, S. Liu, and J. Wang, "Event-triggered adaptive fuzzy approach-based lateral motion control for autonomous vehicles," *IEEE Transactions on Intelligent Vehicles*, vol. 9, p. 1260–1269, Jan. 2024.

[9] A. Norouzi, M. Masoumi, A. Barari, and S. Farrokhpour Sani, "Lateral control of an autonomous vehicle using integrated backstepping and sliding mode controller," *Proceedings of the Institution of Mechanical Engineers, Part K: Journal of Multi-body Dynamics*, vol. 233, p. 141–151, Sept. 2018.

[10] A. Jo, H. Lee, D. Seo, and K. Yi, "Model-reference adaptive sliding mode control of longitudinal speed tracking for autonomous vehicles," *Proceedings of the Institution of Mechanical Engineers, Part D: Journal of Automobile Engineering*, vol. 237, p. 493–515, Feb. 2022.

[11] G. Tagne, R. Talj, and A. Charara, "Higher-order sliding mode control for lateral dynamics of autonomous vehicles, with experimental validation," in *2013 IEEE Intelligent Vehicles Symposium (IV)*, p. 678–683, IEEE, June 2013.

[12] J. Chen, W. Zhan, and M. Tomizuka, "Autonomous driving motion planning with constrained iterative lqr," *IEEE Transactions on Intelligent Vehicles*, vol. 4, p. 244–254, June 2019.

[13] K. Lee, S. Jeon, H. Kim, and D. Kum, "Optimal path tracking control of autonomous vehicle: Adaptive full-state linear quadratic gaussian (lqg) control," *IEEE Access*, vol. 7, p. 109120–109133, 2019.

[14] C. Sun, X. Zhang, Q. Zhou, and Y. Tian, "A model predictive controller with switched tracking error for autonomous vehicle path tracking," *IEEE Access*, vol. 7, p. 53103–53114, 2019.

[15] Z. Zhou, C. Rother, and J. Chen, "Event-triggered model predictive control for autonomous vehicle path tracking: Validation using carla simulator," *IEEE Transactions on Intelligent Vehicles*, vol. 8, p. 3547–3555, June 2023.

[16] T. Qie, W. Wang, C. Yang, Y. Li, Y. Zhang, W. Liu, and C. Xiang, "An improved model predictive control-based trajectory planning method for automated driving vehicles under uncertainty environments," *IEEE Transactions on Intelligent Transportation Systems*, vol. 24, p. 3999–4015, Apr. 2023.

[17] K. Kahraman, M. Senturk, M. T. Emirler, I. M. C. Uygan, B. Aksun-Guvenc, L. Guvenc, and B. Efendioglu, "Yaw stability control system development and implementation for a fully electric vehicle," 2020.

[18] I. The MathWorks, "Matlab (version 9.13.0 r2022b)," 2022.